

Hypoxia Induces Trimethylated H3 Lysine 4 by Inhibition of JARID1A Demethylase

Xue Zhou¹, Hong Sun¹, Haobin Chen¹, Jiri Zavadil², Thomas Kluz¹, Adriana Arita¹, and Max Costa¹

Abstract

Histone H3 lysine 4 (H3K4) trimethylation (H3K4me3) at the promoter region of genes has been linked to transcriptional activation. In the present study, we found that hypoxia (1% oxygen) increased H3K4me3 in both normal human bronchial epithelial Beas-2B cells and human lung carcinoma A549 cells. The increase of H3K4me3 from hypoxia was likely caused by the inhibition of H3K4 demethylating activity, as hypoxia still increased H3K4me3 in methionine-deficient medium. Furthermore, an *in vitro* histone demethylation assay showed that 1% oxygen decreased the activity of H3K4 demethylases in Beas-2B nuclear extracts because ambient oxygen tensions were required for the demethylation reaction to proceed. Hypoxia only minimally increased H3K4me3 in the BEAS-2B cells with knockdown of JARID1A, which is the major histone H3K4 demethylase in this cell line. However, the mRNA and protein levels of JARID1A were not affected by hypoxia. GeneChip and pathway analysis in JARID1A knockdown Beas-2B cells revealed that JARID1A regulates the expression of hundreds of genes involved in different cellular functions, including tumorigenesis. Knocking down of JARID1A increased H3K4me3 at the promoters of *HMOX1* and *DAF* genes. Thus, these results indicate that hypoxia might target JARID1A activity, which in turn increases H3K4me3 at both the global and gene-specific levels, leading to the altered programs of gene expression and tumor progression. *Cancer Res*; 70(10); 4214–21. ©2010 AACR.

Introduction

Cancer cells experience severe hypoxia, resulting from reduced oxygen supply from blood vessels because of the rapid cell proliferation characteristic of solid tumors. Activation of the major transcription factor hypoxia-inducible factor 1 (HIF-1), as well as other important transcription factors such as NF- κ B, activator protein 1, p53, and c-Myc drive a majority of hypoxic gene expressions or repressions (1). This would result in the transcriptional activation of genes that increase angiogenesis, glycolysis, metastasis, and oppose apoptosis. Consequently, this shift in gene expression allows the cancer cell to survive proliferation and metastasis in a hypoxic environment. However, the mechanisms by which cancer cells could activate or repress gene expression remains unclear.

The fundamental unit of chromatin is the nucleosome, which consists of 146 bp of DNA wrapped twice around an octamer formed from two copies of each histone H2A, H2B,

H3, and H4. Histone modifications at NH₂-terminal tails which protrude from the nucleosomes are now recognized as critical epigenetic marks that modulate gene expression and genomic function. At least eight types of histone modifications have been identified. Among them, acetylation, methylation, and phosphorylation have been most studied. These modifications act in combination to modulate chromatin structure and regulate gene expression (2). Generally, H3K9, H3K27, and H4K20 methylation are found in genes that are transcriptionally silent, whereas histone H3 lysine 4 (H3K4), H3K36, and H3K79 methylation are associated with active transcription (3).

Active promoters are marked by H3K4 trimethylation (H3K4me3) and this mark has been linked to transcriptional activation in a variety of eukaryotic species (4–6). H3K4me3 is catalyzed by a group of methyltransferases that contain a SET domain. Demethylation of this site could be reversed by four JARID1 family histone demethylases that are capable of removing the methyl groups from methylated H3K4. The JARID1 family in humans consists of four enzymes: KDM5A/RBP2/JARID1A, KDM5B/PLU-1/JARID1B, and two highly homologous proteins encoded by sex chromosome-specific genes, KDM5C/SMCX/JARID1C, found on the X chromosome, and KDM5D/SMCY/JARID1D, found on the Y chromosome (7–11). These demethylases are members of the dioxygenase superfamily and they require oxygen, iron, and ascorbic acid as essential cofactors to oxidatively demethylate trimethylated H3K4. Thus, they are less active under hypoxic conditions. Because they remove a gene-activating mark, they have been associated with transcriptional repression (11, 12).

Authors' Affiliations: ¹Nelson Institute of Environmental Medicine, New York University School of Medicine, Tuxedo, New York and ²Department of Pathology, NYU Cancer Institute and Center for Health Informatics and Bioinformatics, NYU Langone Medical Center, New York, New York

Note: Supplementary data for this article are available at Cancer Research Online (<http://cancerres.aacrjournals.org/>).

Corresponding Author: Max Costa, Nelson Institute of Environmental Medicine, New York University School of Medicine, 57 Old Forge Road, Tuxedo, NY 10987. Phone: 845-731-3515; Fax: 845-351-2118; E-mail: max.costa@nyumc.org.

doi: 10.1158/0008-5472.CAN-09-2942

©2010 American Association for Cancer Research.

Experimental evidence indicates that individual members of the JARID1 family of H3K4 demethylases have unique functional properties and divergent expression profiles. JARID1A was originally described as a binding partner for the tumor suppressor protein retinoblastoma (RB; ref. 13). JARID1A is distinct from other histone-modifying enzymes in that it has a DNA-binding motif within its AT-rich interaction domain (ARID), and this is essential for its transcriptional regulation and demethylation of H3K4me3 marks (14). JARID1A functions in the regulation of cell differentiation (15). Genome-wide location analysis revealed that JARID1A has a high correlation with H3K4me3 at gene promoters and it regulates two functionally distinct classes of genes: differentiation-independent and differentiation-dependent JARID1A target genes (15, 16). JARID1B has been described as a cancer antigen that is overexpressed in 90% of breast carcinomas (17). Very little is known about the molecular function of JARID1C, with the exception that it escapes X inactivation and is mutated in X-linked mental retardation (18). JARID1D has not yet been associated with any form of human disease.

In this study, we have shown that hypoxia increased H3K4me3 at the global level in A549 and Beas-2B cell lines, and this effect is attributed to the inhibition of the demethylation process, particularly the H3K4 demethylase JARID1A. GeneChip and functional analysis suggested that JARID1A regulates the expression of genes involved in several distinct cellular categories. Knocking down of JARID1A increased H3K4me3 at the promoters of *HMOX1* and *DAF* genes.

Materials and Methods

Cell culture. Cells were grown at 37°C in an incubator with a humidified atmosphere containing 5% CO₂. A549 cells were cultured in F-12K medium (Mediatech, Inc.) and Beas-2B cells were grown in DMEM. Both A549 and Beas-2B cell lines were purchased from American Type Culture Collection. All media were supplemented with 10% fetal bovine serum and 1% penicillin/streptomycin. Cells were exposed to hypoxic conditions in a chamber with a continuous flow of a hypoxic gas mixture with 1% oxygen at 37°C. The levels of oxygen in the chambers were verified using a gas monitor (SKC, Inc.).

Preparation of histones, whole cell lysates, and measurement of HIF-1 α . The cells were 80% to 90% confluent before collection. Histones were extracted from the cells as described previously (19, 20). Whole cell lysates were extracted by incubating with ice-cold radioimmunoprecipitation assay buffer for 20 minutes on ice, followed by centrifugation at 14,000 \times g for 15 minutes. The supernatant was collected and cell extracts for HIF-1 α measurement were prepared as described previously (21). The immunoblottings were performed with HIF-1 α antibody (Novus Biologicals) at 1:500 dilution.

Western blotting. Protein concentrations were determined using the Bio-Rad detergent-compatible protein assay (Bio-Rad), and 5 μ g of histones were separated by 15% SDS-PAGE gel and transferred to polyvinylidene difluoride membranes (Bio-Rad). Immunoblotting was performed using

trimethyl H3K4 (1:5,000; Abcam) primary antibody, and horseradish peroxidase-conjugated anti-rabbit secondary antibody (Santa Cruz Biotechnology). Detection was accomplished by chemical fluorescence following an enhanced chemiluminescence Western blotting protocol (Amersham). After transfer to polyvinylidene difluoride membranes, the gels were stained with Bio-safe Coomassie stain (Bio-Rad) to assess the loading of histones. The immunoblots were scanned and analyzed using ImageJ software, and values were normalized to that obtained in the control sample(s).

Transient transfection of RNAi. Transient transfection of RNAi was done in Beas-2B cells using LipofectAMINE RNAiMAX (Invitrogen) following the protocols of the manufacturer. Seventy-two hours after transfection, the cell extracts were prepared either for Western blotting or semiquantitative reverse transcription-PCR (RT-PCR). JARID1A RNAi was purchased from Invitrogen.

Histone H3K4 demethylation assay. Nuclear extracts were prepared using a CellLytic NuCLEAR extraction kit (Sigma). Freshly prepared nuclear extracts (130 μ g) from Beas-2B cells were incubated with 5 μ g of histones (Upstate) in histone demethylation buffer [50 mmol/L HEPES (pH 8.0), 2 μ g/mL bovine serum albumin, 0.1 mmol/L DL-DTT, 100 μ mol/L FeSO₄, 2 mmol/L ascorbate, 1 mmol/L α -ketoglutarate, and protease inhibitors] in a final volume of 50 μ L at 37°C. Before mixing and incubating in hypoxia, nuclear extracts, histones, histone demethylation buffer, and water were all pre-equilibrated at 1% oxygen atmosphere for 1 hour. The reaction in hypoxia was carried out in a glove box (Biospherix) with 1% oxygen, which was verified using a gas monitor (SKC). Following overnight incubation, the demethylation reaction was terminated by the addition of EDTA to a final concentration of 1 mmol/L. The reaction mixture was analyzed by Western blotting using H3K4me3 antibody. The experiments were carried out in duplicate.

Semiquantitative RT-PCR and real-time RT-PCR. Total RNA was extracted from cells immediately after exposure using Trizol reagent (Invitrogen), and following the protocols of the manufacturer. RNA concentration was determined by absorbance at 260 nm. First-strand cDNA was synthesized using SuperScript III First-Strand Synthesis SuperMix for qRT-PCR (Invitrogen). Semiquantitative PCR was performed using Taq DNA polymerase (Roche) and the specific primers are indicated below: *JARID1A*, 5'-GGAGCCTCTGAGTGATCTGG-3' (forward) and 5'-TCCAATAAGTAGCGAAGCAG-3' (reverse); *COL1A2*, 5'-TTGACCCTAACCAAGGATGC-3' (forward) and 5'-ATGCAATGCTGTTCTTGCAG-3' (reverse); *HMOX1*, 5'-ACATCTATGTGGCCCTGGAG-3' (forward) and 5'-TGTTGGGGAAGGTGAAGAAG-3' (reverse); *β -actin*, 5'-TCACCCACACTGTGCCCATCTACGA-3' (forward) and 5'-CAGCGGAACCGCTCATTGCCAATGG-3' (reverse). Finally, PCR products were visualized by ethidium bromide on 1% agarose gel. Real-time RT-PCR was performed using the 7900HT Fast Real-time PCR System (Applied Biosystems) with Fast SYBR Green Master Mix reagent (Applied Biosystems). Genes were amplified using the following primers: *JARID1A*, 5'-GCTTGGCAATGGGAACAAAA-3 (forward) and 5'-CCGTTGTCTCATTTGCATGTTAA-3

(reverse); *JARID1B*, 5-AGTGCAGTGGCGCATCT-3 (forward) and 5-GGCAGAAGAATTGCTGGAATCTAG-3 (reverse); *JARID1C*, 5-GCAAAAATATTGGCTCCTTGCT-3 (forward) and 5-ACGTGTGTTACTGCACAAGGTT-3 (reverse); *JARID1D*, 5-GCCTAGCTGGGCTGAATTCC-3 (forward) and 5-GATGC-CAGACTTCTCTGCTATGG-3 (reverse); and β -actin, 5-ATCGTCCACCACAAATGCTTCTA-3 (forward) and 5-AGC-CATGCCAATCTCATCTTGT-3 (reverse). All quantifications were normalized to β -actin. cDNA was amplified under the same conditions.

Chromatin immunoprecipitation assays. Beas-2B cells were cross-linked using 37% formaldehyde to a final concentration of 1%. The chromatin immunoprecipitation (ChIP) assay was performed using EZ ChIP Kit (Millipore) according to the protocols of the manufacturer. Antibodies against trimethyl H3K4 (Abcam) and normal IgG were used for immunoprecipitation. Semiquantitative PCR was performed using the specific primers indicated below: *HMOX1*, 5-GAGCCTGCAGCTTCTCAGAT-3 (forward) and 5-AA-CAGCTGATGCCACTTTC-3 (reverse); *DAF*, 5-TAAGCTCC-CACGTGATTCT-3 (forward) and 5-ATTCACCAAGTGTGG-TGTGT-3 (reverse); *DUSP2*, 5-AAAAACGGAGGGGTGCTAGT-3 (forward) and 5-ACCATACAAGGGCAGAGCAG-3 (reverse). PCR products were separated on 2% agarose gels and visualized by ethidium bromide staining.

Results

Hypoxia increases global levels of H3K4me3. To experimentally measure if exposure to hypoxia results in changes in H3K4me3, Beas-2B cells were exposed to hypoxia (1% oxygen). Exposure of BEAS-2B cells to hypoxia for 24 hours increased the global level of H3K4me3. In parallel samples, intracellular HIF-1 α protein levels were found to be increased by hypoxia (Fig. 1A). It was noticed that both isoforms of HIF-1 α which resulted from alternative splicing were present in Beas-2B cells (Fig. 1A), as was previously found in HeLa and A549 cells (22, 23). N-myc downstream-regulated gene 1 (NDRG1), which is strongly upregulated by HIF-1 α under hypoxia (24, 25), was also increased (Fig. 1A).

The hypoxia-induced H3K4me3 was further studied at different time intervals in Beas-2B cells and in A549 cells. Exposure of BEAS-2B cells to hypoxia increased the global level of H3K4me3 at 6 and 48 hours as well as at 24 hours, whereas exposure of A549 cells to hypoxia only increased the global level of H3K4me3 at 6 and 24 hours, but failed to increase H3K4me3 at 48 hours compared with normoxia control (Fig. 1A and B). It should be noted that both cell monolayers were subconfluent and comparable in cell density. We next assessed the level of HIF-1 α to determine if a hypoxic response was initiated in the cancerous A549 cells compared

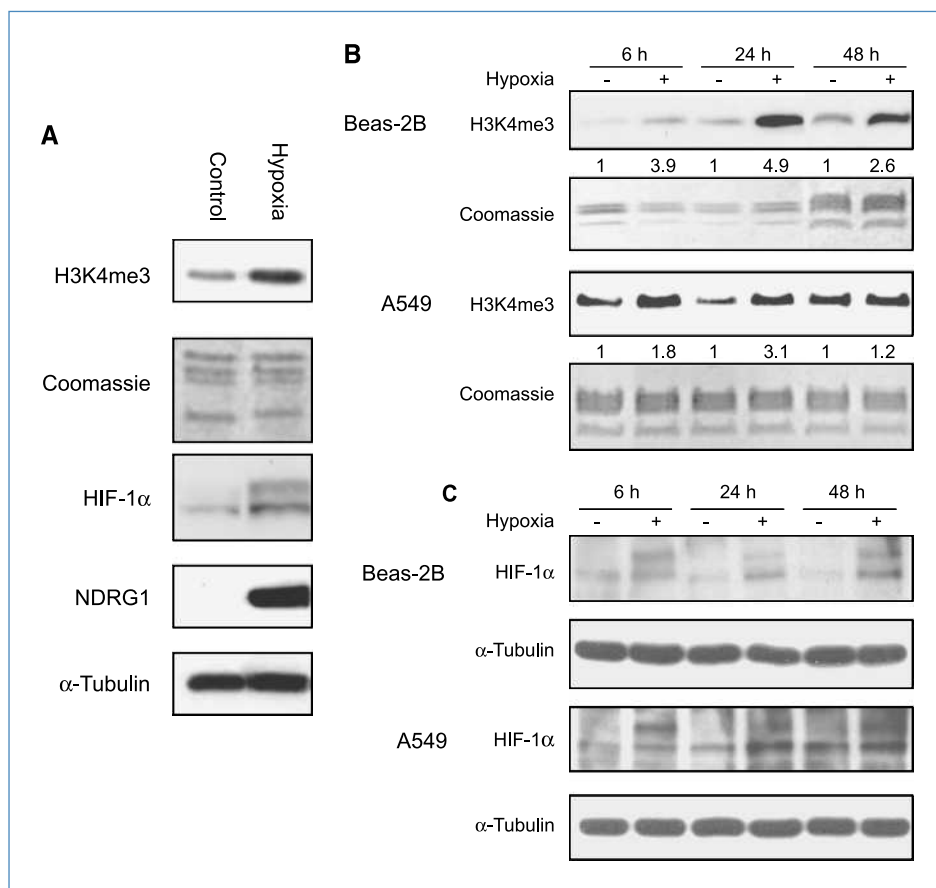


Figure 1. A, Beas-2B cells were exposed to hypoxia (1% oxygen) for 24 hours, and histones were then extracted. H3K4me3 was detected using Western blotting as described in Materials and Methods. In parallel samples, the intracellular HIF-1 α and NDRG1 protein levels were measured using Western blotting. The same membranes were stripped and reprobed with α -tubulin antibody as loading control. B, the effect of hypoxia on H3K4me3 in A549 and Beas-2B cells after 6, 24, and 48 hours of hypoxia exposure. The numbers below the figure represent the relative intensity of the bands. C, the intracellular HIF-1 α protein levels were measured using Western blotting with anti-HIF-1 α antibody after 6, 24, and 48 hours of hypoxia exposure. After HIF-1 α immunoblotting, the same membrane was stripped and reblotted with α -tubulin to assess the protein loading.

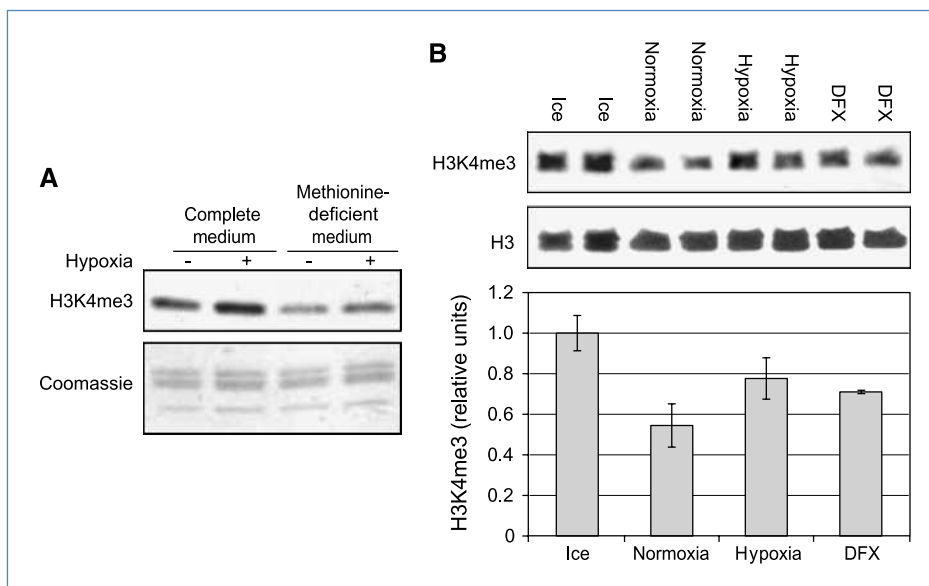


Figure 2. A, Beas-2B cells were seeded with DMEM complete medium. On the second day, cells were preincubated with complete DMEM or methionine-deficient DMEM for 4 hours, and cells were exposed to hypoxia for 24 hours. Histones were extracted and immunoblotted with anti-H3K4me3 antibody. The gel was stained with Coomassie blue as a loading control. The results were repeated in another independent experiment; one representative blot is shown here. B, hypoxia inhibited the activity of histone H3K4 demethylase *in vitro*. The histone H3K4 demethylation assay was performed as described in Materials and Methods. The reaction mixture was incubated on ice, or incubated at 37°C in normoxia, hypoxia (1% oxygen), and in the presence of 1 mmol/L of deferoxamine (DFX) overnight. The same membrane was stripped and reblotted with H3 antibody to verify the loading. Each condition was used in duplicate. The intensity of the bands was quantified, and values were normalized to the samples that were incubated on ice and were plotted in the graph. Error bars represent SD.

with the immortalized normal BEAS-2B cells at the 48-hour time interval. HIF-1 α was induced compared with normoxia after 6, 24, and 48 hours of hypoxia exposure in Beas-2B cells (Fig. 1C). In our previous study, we showed that hypoxia could induce HIF-1 α in A549 cells in a time-dependent manner (23). Here, we showed that hypoxia induced HIF-1 α compared with normoxia only at 6 and 24 hours in A549 cells (Fig. 1C). The HIF-1 α at 48 hours was induced to the same level by both hypoxia and normoxia in A549 cells (Fig. 1C). This suggested that A549 cells maintained at normal oxygen levels became hypoxic at later time intervals (48 hours), which increased H3K4me3 in normoxic A549 cells to the level of H3K4me3 induced by 48 hours of hypoxia (Fig. 1B).

Hypoxia increases H3K4me3 by inhibiting H3K4 demethylating activity. Because methionine is essential for *S*-adenosyl methionine synthesis, which has a short half-life in cells, the withdrawal of methionine in the culture medium leads to a lowered intracellular pool of *S*-adenosyl methionine and a generalized inhibition of methyl transfer reactions. Beas-2B cells were preincubated with complete DMEM or methionine-deficient DMEM for 4 hours, and cells were exposed to hypoxia for 24 hours. Histones were extracted and subjected to Western blotting analysis with antibody directed against trimethylated H3K4. In cells maintained in methionine-deficient medium, the basal level of H3K4me3 was decreased but hypoxia still elevated H3K4me3 compared with untreated cells (Fig. 2A). This result suggested that the removal of histone H3K4 methylation was inhibited by hypoxia.

To further study if hypoxia inhibits the H3K4 demethylase enzyme activity, an *in vitro* histone H3K4 demethylation assay was performed. Histones that contain H3K4me3 were incubated with nuclear extracts from Beas-2B cells at 37°C overnight with or without hypoxia, and were subjected to Western blotting using trimethyl H3K4 antibody. As shown in Fig. 2B, incubation of histones with nuclear extracts overnight at normoxia led to a decrease in trimethyl H3K4 levels at 37°C, compared with the reaction mixture incubated on ice which abolished the demethylase activity. However, the reaction was attenuated by hypoxia, as well as by the addition of iron chelator deferoxamine. The result indicated that hypoxia inhibited H3K4 demethylase activity which likely caused the increase of H3K4me3 in living cells.

By examining the microarray data and the real-time RT-PCR results in wild-type Beas-2B cells, we identified that

Table 1. List of the expression levels (raw data) of *JARID1A*, *JARID1B*, *JARID1C*, and *JARID1D* in the GeneChip in Beas-2B cells

Beas-2B	Probe	Raw
<i>JARID1A</i>	202040_s_at	236.6
<i>JARID1B</i>	201548_s_at	203.8
<i>JARID1C</i>	202383_at	122.3
<i>JARID1D</i>	No hits	

JARID1A is highly expressed in Beas-2B cells (Table 1; Fig. 3A; see Supplementary Table S1 and Supplementary Fig. S1 for A549 cells). To examine the role of *JARID1A* in hypoxia-induced H3K4me3, *JARID1A* mRNA levels were measured in Beas-2B cells following exposure to hypoxia. It was found that hypoxia did not cause any measurable change in *JARID1A* mRNA level at 24 hours (Fig. 3A and B, top). We also examined the effect of hypoxia on the levels of *JARID1A* protein. Beas-2B cells were exposed to hypoxia for 24 hours, and whole cell lysates were isolated and subjected to Western blotting analysis with antibody directed against *JARID1A*. As shown in Fig. 3B (bottom), hypoxia had no effect on *JARID1A* protein levels at 24 hours.

We further knocked down *JARID1A* in Beas-2B cells to see if H3K4me3 could still be increased by hypoxia to the same degree after knocking down *JARID1A*. The knockdown efficiencies of different *JARID1A* RNAs were determined prior to this experiment. As shown in Fig. 3C, *JARID1A* RNAi 1 and 3 have better knockdown efficiencies compared with RNAi 2. To avoid any possible off-target effect, we used both *JARID1A* RNAi 1 and 3. Knocking down of *JARID1A* using

both RNAi oligos increased global H3K4me3, and hypoxia did not further increase H3K4me3 in these cells (Fig. 3D). These results indicated that hypoxia increased H3K4me3 by inhibiting the demethylating process, in particular, the *JARID1A* H3K4 demethylase.

Modulation of gene expression by *JARID1A* in Beas-2B cells. Because *JARID1A* is very important in hypoxia-induced H3K4me3, we next used the GeneChip microarray to study which genes were regulated by *JARID1A*. Gene expression arrays were performed using Affymetrix GeneChip in wild-type and *JARID1A* knockdown cells. The GeneSpring 7.0 program (Silicon Genetics) was used to filter gene expression levels. Results were visualized using a Venn diagram, and known genes whose expression levels exhibited changes of at least 2-fold ($P < 0.05$) upon *JARID1A* knockdown were listed in Supplementary Tables S2 and S3. There were 91 genes upregulated (Supplementary Table S2) and 291 genes downregulated (Supplementary Table S3) when *JARID1A* was knocked down.

To validate the GeneChip data, the expression levels of selected differentially expressed genes were assessed by

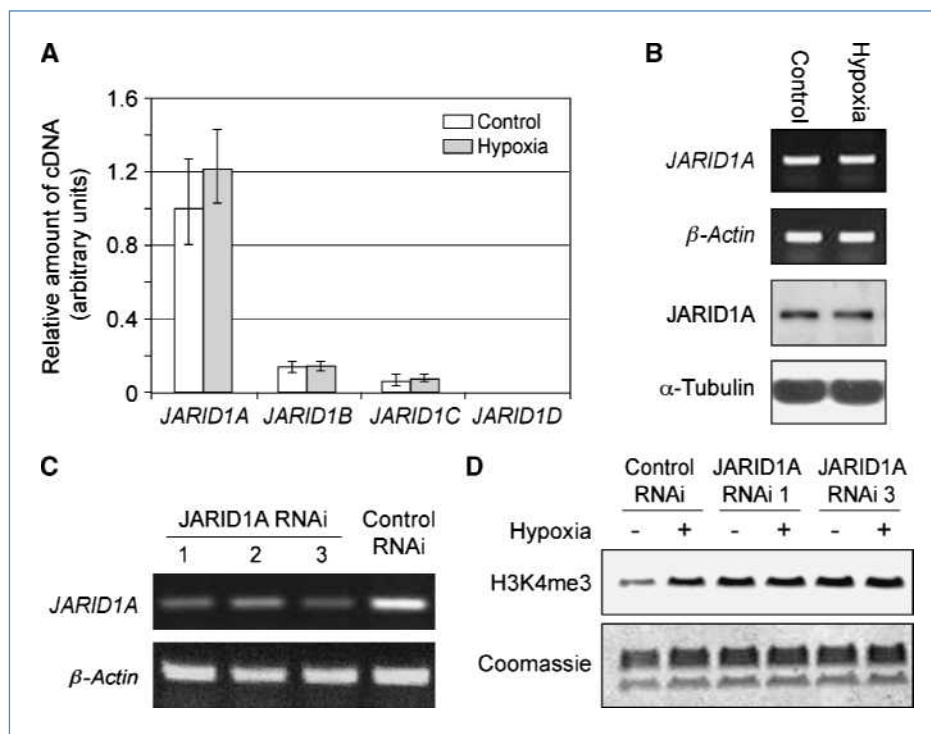


Figure 3. A, real-time RT-PCR analysis of the relative mRNA expression levels of *JARID1A*, *JARID1B*, *JARID1C*, and *JARID1D* in control (white) and 24 hours hypoxia (gray) treated Beas-2B cells. The experiments were done in triplicate. Error bars represent SD. B, Beas-2B cells were exposed to hypoxia. After 24 hours, mRNA was extracted and whole cell lysates were collected. Semiquantitative RT-PCR was then performed using *JARID1A* primers. The cDNA product was visualized in the 1% agarose gels using ethidium bromide staining. β -Actin was used as a loading control. *JARID1A* protein level was analyzed by Western blotting with antibody against *JARID1A*. The same membrane was stripped and reblotted with α -tubulin to assess the protein loading. The results were repeated in another independent experiment; one representative blot is shown here. C, *JARID1A* was knocked down in Beas-2B cells. Seventy-two hours after *JARID1A* RNAi transfection, cells were collected and total mRNA was extracted. Semiquantitative RT-PCR was then performed using *JARID1A* primers. The cDNA product was visualized in the 1% agarose gels using ethidium bromide staining. β -Actin was used as a loading control. D, H3K4me3 was not increased by 24 hours of hypoxia exposure in *JARID1A* knockout cells. Forty-eight hours after *JARID1A* RNAi transfection, cells were exposed to hypoxia for 24 hours. Histones were extracted and immunoblotted with anti-H3K4me3 antibody. The gel was stained with Coomassie blue as a loading control. The results were repeated in another independent experiment; one representative blot is shown here.

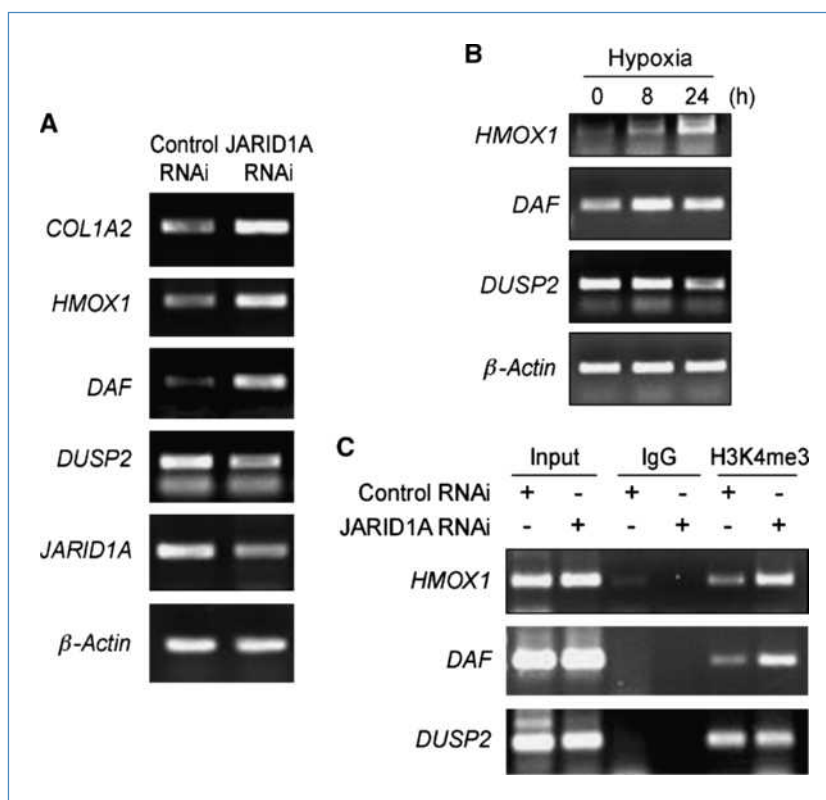


Figure 4. A, semiquantitative RT-PCR analysis of four differentially expressed genes in Beas-2B cells. After 72 hours of JARID1A RNAi transfection, cells were collected and total mRNA was extracted. Semiquantitative RT-PCR was then performed. The PCR-amplified cDNA was separated by 1% agarose gel electrophoresis containing ethidium bromide. β -Actin was used as a loading control. B, semiquantitative RT-PCR analyses of *HMOX1*, *DAF*, and *DUSP2* genes in Beas-2B cells. After 8 or 24 hours of hypoxia exposure, cells were collected and total mRNA was extracted. Semiquantitative RT-PCR was then performed. The PCR-amplified cDNA was separated by 1% agarose gel electrophoresis containing ethidium bromide. β -Actin was used as a loading control. C, knocking down of JARID1A induced enrichment of H3K4me3 in *HMOX1* and *DAF* promoters in Beas-2B. After 72 hours of JARID1A RNAi transfection, the ChIP assays were performed using trimethyl H3K4 antibody. Normal rabbit IgG was used as a negative control. The specific primers were used for the PCR amplification as indicated in Materials and Methods.

semiquantitative RT-PCR (Fig. 4A). These included three upregulated genes (*COL1A2*, *HMOX1*, and *DAF*) and one downregulated gene (*DUSP2*). The results were consistent with the GeneChip findings.

Pathway analysis of differentially regulated genes in JARID1A knockdown Beas-2B cells. To gain further information into the biological functions of the JARID1A-regulated genes, we classified the genes by using three different pathway databases: KEGG, BIOCARTA, and Func Anot. The significant ($P < 0.05$) KEGG pathway involved in the 91 commonly upregulated genes was the insulin signaling pathway, and among the 291 downregulated genes, the significant ($P < 0.05$) KEGG pathways involved were the regulation of actin cytoskeleton, focal adhesion, p53 signaling pathway, melanoma, and extracellular matrix–receptor interaction. In the BIOCARTA categories, signal transduction through IL-1R, Fc ϵ receptor I signaling in mast cells, links between Pyk2 and mitogenactivated protein kinases, oxidative stress–induced gene expression via Nrf2, angiotensin II–mediated activation of JNK pathways via Pyk2-dependent signaling, the role of MAL in Rho-mediated activation of SRFm, and keratinocyte differentiation were observed in 91 upregulated genes, whereas

only the CXCR4 signaling pathway was found in downregulated genes ($P < 0.05$). The complete list and functional categories of the differentially expressed genes by JARID1A knockdown in the Beas-2B cell line are in Supplementary Table S4.

Knocking down of JARID1A induces H3K4me3 at the HMOX1 and DAF promoters in Beas-2B cells. We next knocked down JARID1A to study whether the level of H3K4me3 at the promoters of specific genes was increased using a ChIP assay. We analyzed two upregulated genes, heme oxygenase-1 (*HMOX1*) and decay-accelerating factor (*DAF* or *CD55*), and one downregulated gene, dual-specificity phosphatase 2 (*DUSP2*) from the JARID1A knockdown GeneChip results. *HMOX1* catalyzes the oxidative catabolism of heme to form biliverdin and CO, and it is proposed to protect cells or tissues from oxidative injury (26–29). *DAF* exists in most of the malignant tumors, and it functions as an inhibitor of the complement system (for review, see ref. 30). *DUSP2* dephosphorylates ERK and p38, which positively regulates the inflammatory response (for review, see ref. 31). It should be noted that the mRNA of *HMOX1* and *DAF* were increased by hypoxia, and the mRNA of *DUSP2* was decreased by hypoxia (Fig. 4B). The lower bands are probably due to primer

self-extension. As shown in Fig. 4C, knocking down of JARID1A increased the amount of H3K4me3 transcription-activating mark at *HMOX1* and *DAF* promoters, but not H3K4me3 at the *DUSP2* promoter.

Discussion

Several studies have indicated that hypoxia was able to alter epigenetic homeostasis and that these changes might play a role in promoting tumorigenesis. It has been shown that hypoxia increased localized histone acetylation surrounding activated genes (32–34). Studies from our lab have shown that dimethylated H3K9 was elevated following hypoxia exposure, and this effect was mediated by the increase of G9a methyltransferase protein and enzyme activity, as well as by inhibiting histone H3K9 demethylases (23). In addition, dimethylated H3K9 at the promoters of hypoxia-repressed genes, *MLH1* and *DHFR*, were found to be increased by hypoxia. A more recent study has investigated changes in histone methylation on HIF target genes when cells are challenged with hypoxia (32). In that study, the promoters of the hypoxia-induced genes, *VEGF* and *EGRI*, and repressed genes, *AFP* and *ALB*, were investigated. When cells were exposed to hypoxia, there was an observed increase of H3K4me3 and a decrease of H3K27 trimethylation in all the promoters of genes, regardless of whether they were activated or repressed. However, the mechanisms and identity of the methylases and demethylases involved in this modification remain unclear. In the present study, we also found that exposure of Beas-2B cells to hypoxia increased H3K4me3 at 6, 24, and 48 hours, and exposure of A549 cells to hypoxia increased H3K4me3 at 6 and 24 hours. At 48 hours, however, the H3K4me3 in the normoxic A549 cells was higher and hypoxia failed to increase H3K4me3 compared with control. We attributed this to oxygen deprivation in the medium of untreated A549 cells at later time intervals (48 hours), which made the cells hypoxic and increased H3K4me3 due to the demethylase inhibition. In 1973, Goldblatt and collaborators (35) observed that rat embryo cells grown for a prolonged period *in vitro* developed some degree of hypoxia due to insufficient diffusion of ambient oxygen into the stationary layer of the medium and this hypoxia caused malignant transformation. A549, as a cancerous cell line, forms clusters at higher density whereas Beas-2B cells do not have this growth pattern (Supplementary Fig. S2). Therefore, A549 cells, at a later time interval, likely developed pericellular hypoxia because of their growth pattern.

To study the mechanisms by which hypoxia increase H3K4me3, a transcriptional activating mark in chromatin, Beas-2B cells were preincubated in the methionine-deficient medium prior to exposure to hypoxia. Our data suggested that hypoxia increased H3K4me3 by inhibiting the demethylating activity rather than activating the methylating enzymes, as was evident from the finding that hypoxia still increased H3K4me3 when the intracellular methylation process was suppressed by the absence of methionine. *In vitro* histone H3K4 demethylation assay further confirmed that

hypoxia inhibited the enzymatic activity of the demethylases targeting trimethyl H3K4, therefore preventing the removal of the methyl group from H3K4me3 and increasing the trimethylation levels of H3K4. As a major trimethylated H3K4 demethylase, the role of JARID1A in hypoxia-induced H3K4me3 was investigated. Our results suggested that hypoxia did not affect JARID1A mRNA and protein level. These results are contradictory to the findings by Xia and coworkers (36). In their study, *JARID1A* mRNA was found to be upregulated in HepG2 cells by hypoxia and in glioblastoma multiforme (36). The conflicting observations were likely due to the different hypoxic conditions and cell lines (or tumor tissue). In their study, HepG2 cells were exposed to more severe hypoxia (0.5%) for 4, 8, and 12 hours and mRNA expression levels were determined by Affymetrix GeneChip. The mRNA levels were analyzed in glioblastoma following 0.5% hypoxia challenge. Our study was done by semiquantitative RT-PCR in Beas-2B cells exposed to hypoxia (1%) for 24 hours. Xia's GeneChip results were not confirmed by RT-PCR. In addition to *JARID1A*, *JARID1B* and *JARID1C* are also expressed in Beas-2B cells. However, they might not function and bind to the promoters of the genes in Beas-2B under our experimental conditions, although they could be inhibited by hypoxia. This is supported by our result that hypoxia did not further increase H3K4me3 in the Beas-2B cells after knockdown of JARID1A. This might suggest that JARID1A is the predominant demethylase regulating global H3K4me3 level in the cell lines used in the present study. It is likely that the "open" chromatin structure created by an increase of H3K4me3 at the promoters facilitates the recruitment of HIF to their target genes under hypoxic conditions.

To identify the genes regulated by JARID1A, we used a GeneChip microarray technique following the knockdown of JARID1A in Beas-2B cells. It was expected that knocking down of JARID1A should increase the expression of genes because this inhibits the removal of the methyl groups from the transcription-activating mark H3K4me3, resulting in a higher level of gene expression. However, more genes were downregulated than upregulated by JARID1A knockdown in our study. This might be due to the indirect effect of JARID1A in regulating gene expression, as is confirmed by the ChIP assay, in which H3K4me3 at the promoter of *DUSP2*, the most downregulated gene (7.5-fold) in the GeneChip assay, were not altered when JARID1A was knocked down (Fig. 4C).

JARID1A preferentially binds to DNA through the CCGCCC motif (14). We identified several CCGCCC sequences in the promoters of *HMOX1* and *DAF*. Therefore, it is likely that JARID1A binds directly to the promoters of *HMOX1* and *DAF*. However, we identified several JARID1A-binding sites at the promoter region of *DUSP2* as well, but JARID1A knockdown had no effect on the H3K4me3 level at this promoter site. The reason could be that the JARID1A binding motif only has six bases and its short length might limit its specificity.

In conclusion, this study suggests that hypoxia exposure is able to induce global as well as gene-specific H3K4me3, which plays an important role in altering gene expression

during hypoxia. We propose that the increase of H3K4me3 induced by hypoxia may be due to inhibition of only one of the H3K4 demethylases, JARID1A. Knocking down of JARID1A, which mimics the inactivation of JARID1A by hypoxia, induced H3K4me3 at the promoters of *HMOX1* and *DAF* genes. Further studies will be directed to investigate which gene promoters are associated with altered H3K4me3 in the genome and the extent of changes in the amount of this modification that is induced by hypoxia using ChIP-seq, and perform ChIP-seq with JARID1A antibody following similar treatment with hypoxia to correlate the changes in H3K4me3 with the location of JARID1A.

References

- Kenneth NS, Rocha S. Regulation of gene expression by hypoxia. *Biochem J* 2008;414:19–29.
- Strahl BD, Allis CD. The language of covalent histone modifications. *Nature* 2000;403:41–5.
- Peterson CL, Laniel MA. Histones and histone modifications. *Curr Biol* 2004;14:R546–51.
- Martin C, Zhang Y. The diverse functions of histone lysine methylation. *Nat Rev Mol Cell Biol* 2005;6:838–49.
- Mikkelsen TS, Ku M, Jaffe DB, et al. Genome-wide maps of chromatin state in pluripotent and lineage-committed cells. *Nature* 2007;448:553–60.
- Heintzman ND, Stuart RK, Hon G, et al. Distinct and predictive chromatin signatures of transcriptional promoters and enhancers in the human genome. *Nat Genet* 2007;39:311–8.
- Christensen J, Agger K, Cloos PA, et al. RBP2 belongs to a family of demethylases, specific for tri- and dimethylated lysine 4 on histone 3. *Cell* 2007;128:1063–76.
- Iwase S, Lan F, Bayliss P, et al. The X-linked mental retardation gene *SMCX/JARID1C* defines a family of histone H3 lysine 4 demethylases. *Cell* 2007;128:1077–88.
- Klose RJ, Yan Q, Tothova Z, et al. The retinoblastoma binding protein RBP2 is an H3K4 demethylase. *Cell* 2007;128:889–900.
- Seward DJ, Cubberley G, Kim S, et al. Demethylation of trimethylated histone H3 Lys4 *in vivo* by JARID1 JmjC proteins. *Nat Struct Mol Biol* 2007;14:240–2.
- Kim TD, Shin S, Janknecht R. Repression of Smad3 activity by histone demethylase *SMCX/JARID1C*. *Biochem Biophys Res Commun* 2008;366:563–7.
- Pasini D, Hansen KH, Christensen J, Agger K, Cloos PA, Helin K. Coordinated regulation of transcriptional repression by the RBP2 H3K4 demethylase and Polycomb-Repressive Complex 2. *Genes Dev* 2008;22:1345–55.
- Defeo-Jones D, Huang PS, Jones RE, et al. Cloning of cDNAs for cellular proteins that bind to the retinoblastoma gene product. *Nature* 1991;352:251–4.
- Tu S, Teng YC, Yuan C, et al. The ARID domain of the H3K4 demethylase RBP2 binds to a DNA CCGCC motif. *Nat Struct Mol Biol* 2008;15:419–21.
- Benevolenskaya EV, Murray HL, Branton P, Young RA, Kaelin WG, Jr. Binding of pRB to the PHD protein RBP2 promotes cellular differentiation. *Mol Cell* 2005;18:623–35.
- Lopez-Bigas N, Kisiel TA, Dewaal DC, et al. Genome-wide analysis of the H3K4 histone demethylase RBP2 reveals a transcriptional program controlling differentiation. *Mol Cell* 2008;31:520–30.
- Barrett A, Madsen B, Copier J, et al. PLU-1 nuclear protein, which is upregulated in breast cancer, shows restricted expression in normal human adult tissues: a new cancer/testis antigen? *Int J Cancer* 2002;101:581–8.
- Jensen LR, Amende M, Gurok U, et al. Mutations in the JARID1C gene, which is involved in transcriptional regulation and chromatin remodeling, cause X-linked mental retardation. *Am J Hum Genet* 2005;76:227–36.
- Chen H, Ke Q, Kluz T, Yan Y, Costa M. Nickel ions increase histone H3 lysine 9 dimethylation and induce transgene silencing. *Mol Cell Biol* 2006;26:3728–37.
- Zhou X, Sun H, Ellen TP, Chen H, Costa M. Arsenite alters global histone H3 methylation. *Carcinogenesis* 2008;29:1831–6.
- Davidson TL, Chen H, Di Toro DM, D'Angelo G, Costa M. Soluble nickel inhibits HIF-prolyl-hydroxylases creating persistent hypoxic signaling in A549 cells. *Mol Carcinog* 2006;45:479–89.
- Gothie E, Richard DE, Berra E, Pages G, Pouyssegur J. Identification of alternative spliced variants of human hypoxia-inducible factor-1 α . *J Biol Chem* 2000;275:6922–7.
- Chen H, Yan Y, Davidson TL, Shinkai Y, Costa M. Hypoxic stress induces dimethylated histone H3 lysine 9 through histone methyltransferase G9a in mammalian cells. *Cancer Res* 2006;66:9009–16.
- Cangul H. Hypoxia upregulates the expression of the NDRG1 gene leading to its overexpression in various human cancers. *BMC Genet* 2004;5:27.
- Ellen TP, Ke Q, Zhang P, Costa M. NDRG1, a growth and cancer related gene: regulation of gene expression and function in normal and disease states. *Carcinogenesis* 2008;29:2–8.
- Tenhunen R, Marver HS, Schmid R. The enzymatic conversion of heme to bilirubin by microsomal heme oxygenase. *Proc Natl Acad Sci U S A* 1968;61:748–55.
- Otterbein LE, Kolls JK, Mantell LL, Cook JL, Alam J, Choi AM. Exogenous administration of heme oxygenase-1 by gene transfer provides protection against hyperoxia-induced lung injury. *J Clin Invest* 1999;103:1047–54.
- Poss KD, Tonegawa S. Reduced stress defense in heme oxygenase 1-deficient cells. *Proc Natl Acad Sci U S A* 1997;94:10925–30.
- Vile GF, Basu-Modak S, Waltner C, Tyrell RM. Heme oxygenase 1 mediates an adaptive response to oxidative stress in human skin fibroblasts. *Proc Natl Acad Sci U S A* 1994;91:2607–10.
- Mikesch JH, Buerger H, Simon R, Brandt B. Decay-accelerating factor (CD55): a versatile acting molecule in human malignancies. *Biochim Biophys Acta* 2006;1766:42–52.
- Keyse SM. Dual-specificity MAP kinase phosphatases (MKPs) and cancer. *Cancer Metastasis Rev* 2008;27:253–61.
- Johnson AB, Denko N, Barton MC. Hypoxia induces a novel signature of chromatin modifications and global repression of transcription. *Mutat Res* 2008;640:174–9.
- Wang F, Zhang R, Beischlag TV, Muchardt C, Yaniv M, Hankinson O. Roles of Brahma and Brahma/SWI2-related gene 1 in hypoxic induction of the erythropoietin gene. *J Biol Chem* 2004;279:46733–41.
- Jung JE, Lee HG, Cho IH, et al. STAT3 is a potential modulator of HIF-1-mediated VEGF expression in human renal carcinoma cells. *FASEB J* 2005;19:1296–8.
- Goldblatt H, Friedman L, Cechner RL. On the malignant transformation of cells during prolonged culture under hypoxic conditions *in vitro*. *Biochem Med* 1973;7:241–52.
- Xia X, Lemieux ME, Li W, et al. Integrative analysis of HIF binding and transactivation reveals its role in maintaining histone methylation homeostasis. *Proc Natl Acad Sci U S A* 2009;106:4260–5.

Disclosure of Potential Conflicts of Interest

No potential conflicts of interest were disclosed.

Grant Support

ES014454, ES005512, and ES000260 from the National Institutes of Environmental Health Sciences, and CA16087 from the National Cancer Institute.

The costs of publication of this article were defrayed in part by the payment of page charges. This article must therefore be hereby marked *advertisement* in accordance with 18 U.S.C. Section 1734 solely to indicate this fact.

Received 08/07/2009; revised 02/09/2010; accepted 03/04/2010; published OnlineFirst 04/20/2010.

Cancer Research

The Journal of Cancer Research (1916–1930) | The American Journal of Cancer (1931–1940)

Hypoxia Induces Trimethylated H3 Lysine 4 by Inhibition of JARID1A Demethylase

Xue Zhou, Hong Sun, Haobin Chen, et al.

Cancer Res 2010;70:4214-4221. Published OnlineFirst April 20, 2010.

Updated version

Access the most recent version of this article at:
doi:[10.1158/0008-5472.CAN-09-2942](https://doi.org/10.1158/0008-5472.CAN-09-2942)

Supplementary Material

Access the most recent supplemental material at:
<http://cancerres.aacrjournals.org/content/suppl/2010/04/20/0008-5472.CAN-09-2942.DC1>

Cited articles

This article cites 36 articles, 10 of which you can access for free at:
<http://cancerres.aacrjournals.org/content/70/10/4214.full#ref-list-1>

Citing articles

This article has been cited by 13 HighWire-hosted articles. Access the articles at:
<http://cancerres.aacrjournals.org/content/70/10/4214.full#related-urls>

E-mail alerts

[Sign up to receive free email-alerts](#) related to this article or journal.

Reprints and Subscriptions

To order reprints of this article or to subscribe to the journal, contact the AACR Publications Department at pubs@aacr.org.

Permissions

To request permission to re-use all or part of this article, use this link
<http://cancerres.aacrjournals.org/content/70/10/4214>.
Click on "Request Permissions" which will take you to the Copyright Clearance Center's (CCC) Rightslink site.